as external reference) shows a peak at 33.8 ppm; this high-field chemical shift, with respect to other six-coordinate cadmium oxygen derivatives, is in agreement with the data reported for Cd carboxylates.[12]

Hydrolysis experiments have been conducted in 0.1 M solution of 1 in tetrahydrofurane with hydrolysis ratio (h = $[H_2O]$:[1]) varying from 1 to 17. Sols (for h = 1-3), gels (for h = 4-6), or precipitates (for h = 7-17) are successively formed. The infrared spectra show that the acetate ligands remain coordinated ($\nu_{as}(CO_2)$ 1570 cm^{-1}, $\nu_s(CO_2)$ 1423 cm^{-1}), and thus even if the hydrolysis is performed in the presence of an excess of water (h = 17, Figure 1b), the precipitate is solvated (ν(OH) 3290 cm^{-1}, δ(OH) 1618 cm^{-1}). Analytical data establish that the stoichiometry between the two metals is unchanged in the solid 2 isolated for h = 12, as compared to the Cd:Nb stoichiometry of the parent heterometallic molecular precursor 1.

Thermal analysis curves under nitrogen are given in Figure 3. No significant weight loss is observed below 100 °C. TGA and IR spectroscopy show that the acetate ligands are removed between 250 and 450 °C, while the last weight loss (~580 °C) corresponds to the elimination of hydroxyl residues. The rather high temperature at which this phenomenon occurs suggests that these organic groups are bonded to the oxide network. X-ray diffraction experiments performed with a heating chamber show that crystallization of the powder occurs around 600 °C, giving $CdNb_2O_6$ as the only product[13] (Figure 4).

The formation of $CdNb_2O_6$ by chemical routes occurs at quite a low temperature. The $CdNb_2O_6$ ceramic displays a columbite type structure, all metals are thus six-coordinated, with a $[(NbO_6)(CdO_6)(NbO_6)]_\infty$ arrangement. The molecular precursor 1 has an open-shell structure; hydrolysis-polycondensation reactions are likely to occur via the alkoxide ligands. The acetate ligands are still present in the material resulting from hydrolysis; their $\nu(CO_2)$ stretching frequency in the IR are only slightly modified with respect to 1, thus suggesting only limited modification of the cadmium-niobium oxygen core.

Acknowledgment. Financial support from the CNRS is gratefully acknowledged. We thank Dr. F. Chaput (Ecole Polytechnique, Palaiseau) for the powder X-ray diffraction experiments.

Supplementary Material Available: Tables of crystal data, positional coordinates, bond distances and angles, and anisotropic thermal parameters (5 pages); table of calculated and observed F factors for 1 (11 pages). Ordering information is given on any current masthead page.

(12) Rodesiler, P. F.; Amma, E. L. *J. Chem. Soc., Chem. Commun.* **1982**, 182.
(13) Emmenegger, F.; Petermann, A. *J. Cryst. Growth* **1968**, *2*, 33.

Synthesis and Characterization of $K_4Cu_8Te_{11}$: A Novel Solid-State Chalcogenide Compound with a Dodecahedral Cluster as a Building Block

Younbong Park and Mercouri G. Kanatzidis*

Department of Chemistry and Center for Fundamental Materials Research Michigan State University East Lansing, Michigan 48824

Received June 27, 1991

The past decade has stimulated considerable interest for new materials with novel electrical, optical, and catalytic properties. We have been exploring new ternary solid-state metal-chalcogenide compounds using molten salt synthetic methods and particularly the use of alkali-metal polychalcogenide fluxes. We have been successful in synthesizing novel structural types of (poly)sulfides and (poly)selenides of various transition metals at intermediate temperatures ($150 < T < 500$ °C).[1] Recently, we extended our investigations into the polytelluride melts and have discovered several new compounds with unusual structures.[2] Studies on metal tellurides are relatively rare compared to the corresponding sulfides and selenides.[3] Here we report the synthesis of $K_4Cu_8Te_{11}$, a novel tellurium-rich phase, with a complicated three-dimensional structure. Prior to our work there were only four known phases in the A/Cu/Te (A = alkali metal) system, $NaCu_3Te_2$,[4] KCu_3Te_2,[5] NaCuTe,[6] and KCuTe,[6b] all of which contain monotelluride ligands.

The reaction of 0.309 g (1.5 mmol) of K_2Te, 0.064 g (1.0 mmol) of Cu, and 0.765 g (6.0 mmol) of Te in an evacuated Pyrex tube at 350 °C for 3 days followed by 2 °C/h cooling to 100 °C afforded black needle crystals of $K_4Cu_8Te_{11}$ contaminated with a small amount of elemental tellurium. A quantitative analysis on a large number of these crystals performed with scanning electron microscopy/EDS system gave composition $KCu_{2.1}Te_{2.7}$.[7] The product was isolated by removing the excess K_2Te_x with dimethylformamide (DMF) under inert atmosphere. This compound is insoluble in all common organic solvents and relatively stable in water and air. The nature of this material was established by a single-crystal X-ray diffraction study.[8]

The structure of $K_4Cu_8Te_{11}$ is a unique three-dimensional Cu/Te framework with large tunnels running parallel to the crystallographic b axis, as shown in Figure 1. The tunnels are filled with K^+ ions. The framework contains tetrahedral Cu^+ centers bonded to Te^{2-} and Te_2^{2-} ligands. The formula unit can be represented as $K_4Cu_8(Te_2)_5Te$. The structure is somewhat complicated with its three dimensionality, but it is tailored from fused and linked recognizable Cu/Te clusters. The basic building block of this framework is the remarkable pentagonal dodecahedral cluster, $Cu_8(Te_2)_6$, shown in Figure 2A. A remarkable feature of the dodecahedral $Cu_8(Te_2)_6$ cluster is the encapsulation of a K^+ ion in its center. This dodecahedral cluster is made of fused Cu_2Te_3 pentagonal

(1) (a) Kanatzidis, M. G. *Chem. Mater.* **1990**, *2*, 353-363. (b) Kanatzidis, M. G.; Park, Y. *J. Am. Chem. Soc.* **1989**, *111*, 3767-3769. (c) Kanatzidis, M. G.; Park, Y. *Chem. Mater.* **1990**, *2*, 99-101. (d) Park, Y.; Kanatzidis, M. G. *Angew. Chem., Int. Ed. Engl.* **1990**, *29*, 914-915.
(2) (a) Park, Y.; Degroot, D. C.; Schnider, J.; Kannewurf, C.; Kanatzidis, M. G. *Angew. Chem., Int. Ed. Engl.*, in press. (b) Park, Y.; Kanatzidis, M. G., manuscript in preparation.
(3) (a) Kanatzidis, M. G. *Comm. Inorg. Chem.* **1990**, *10*, 161-195. (b) Böttcher, P. *Angew. Chem., Int. Ed. Engl.* **1988**, *27*, 759-772 and references therein. (c) Ansari, M. A.; Ibers, J. A. *Coord. Chem. Rev.* **1990**, *100*, 223-266. (d) Kolis, J. W. *Coord. Chem. Rev.* **1990**, *105*, 195-219. (e) Bernstein, J.; Hoffmann, R. *Inorg. Chem.* **1985**, *24*, 4100-4108. (f) Hulliger, F. *Structural Chemistry of Layer-Type Phases*; Levy, F., Ed.; Reidel: Dordrecht, Netherlands, 1976.
(4) Savelsberg, G.; Schäfer, H. *Mater. Res. Bull.* **1981**, *16*, 1291-1297.
(5) Klepp, K. O. *J. Less-Common Met.* **1987**, *128*, 79-89.
(6) (a) Park, Y.; Kanatzidis, M. G., unpublished results. (b) Savelsberg, G.; Schäfer, H. *Z. Naturforsch.* **1978**, *33b*, 370-373.
(7) This ratio was calibrated by using known K/Cu/Te compounds within 3% error; see ref 2a.
(8) Crystal data for $K_4Cu_8Te_{11}$: monoclinic $C2/m$ (No. 12), Z = 4, a = 24.086 (3) Å, b = 6.821 (6) Å, c = 18.461 (3) Å, β = 124.45 (1)°, V = 1225.0 (4) Å^3, $2\theta_{max}$ (Mo Kα) = 50°. Number of data measured: 2535. Number of data having $F_o^2 > 3\sigma(F_o^2)$: 2029. Number of variables: 121. Number of atoms: 17. μ = 200 cm^{-1}. Final R = 0.025 and R_w = 0.037. As an empirical absorption correction DIFABS was applied to the data set: Walker, N.; Stuart, D. *Acta Crystallogr.* **1983**, *39A*, 158-166. The homogeneity of the product was confirmed by comparing the experimental and calculated (based on the single-crystal structure) X-ray powder diffraction patterns.

0897-4756/91/2803-0781$02.50/0

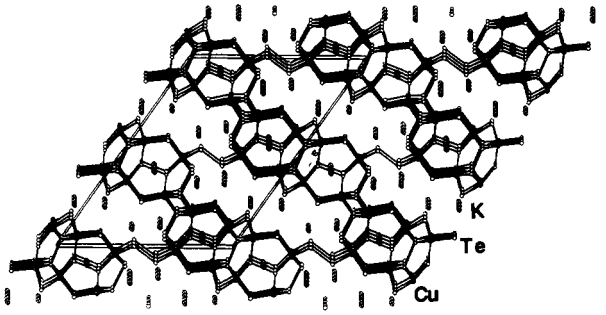

Figure 1. ORTEP representation of the unit cell of $K_4Cu_8Te_{11}$ viewed down the [010] direction. Large crossed circles are K^+ ions. Small open circles are Te atoms and solid circles are Cu atoms.

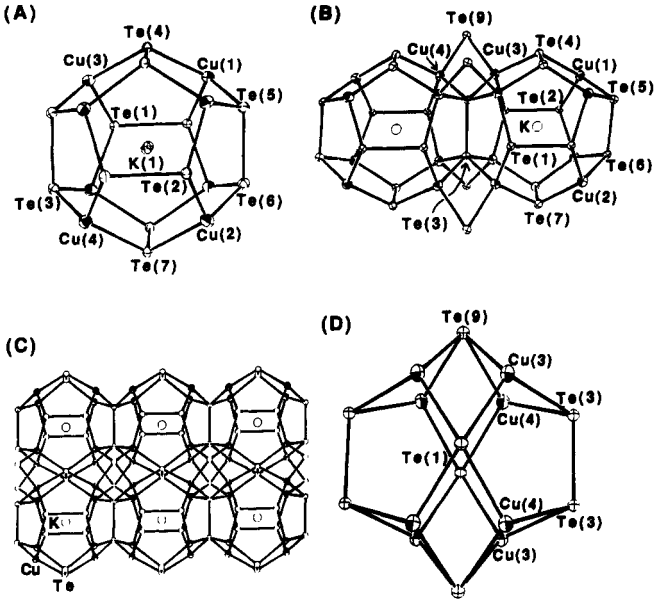

Figure 2. ORTEP representation and labeling scheme of (A) the $[KCu_8Te_{12}]$ dodecahedral cluster (this cluster posseses crystallographic mirror symmetry. The mirror passes through the Te(1), Te(2), and K atoms), (B) two edge-shared $[KCu_8Te_{12}]$ units and the bridging positions of capping Te^{2-} ions, (C) a one-dimensional column of edge-shared double clusters, and (D) the empty Cu_8Te_8 cluster formed by and capped with two monotellurides.

planar five-membered rings each with one ditelluride edge. These $Cu_8(Te_2)_6$ clusters contain three mutually perpendicular sets of ditelluride units. Two dodecahedral $Cu_8(Te_2)_6$ clusters share one Te–Te edge to form a "Siamese twin" type double cluster shown in Figure 2B. These double clusters then share opposite Te–Te edges to form a straight one-dimensional column with oval cross-section, as shown in Figure 2C. The Cu atoms in these columns are bridged by quadruply bonded μ_4-Te^{2-} ions above and below the columns. This results in another unusual Cu_8Te_8 cluster as shown in Figure 2D. This smaller cluster is made of four pentagonal Cu_2Te_3 five-membered rings and eight puckered Cu_2Te_2 four-membered rings. The inside of this Cu_8Te_8 cluster is completely empty with dimensions of 4.062 Å × 6.821 Å × 8.068 Å, corresponding to the distances of Te(1)–Te(1), Te(3)–Te(3), and Te(9)–Te(9), respectively. The one-dimensional columns are then assembled side by side through intercolumn Te–Cu bonding interactions to form Cu/Te layers as shown in Figure 3. The Te atoms participating in these interactions are the Te(6) atoms from the ditelluride Te(5)–Te(6), in the dodecahedral $Cu_8(Te_2)_6$ cluster, which are not edge-shared. The Cu/Te layers are then connected to each other via bridging ditellurides (i.e., Te(8)–Te(8)) that act as pillars

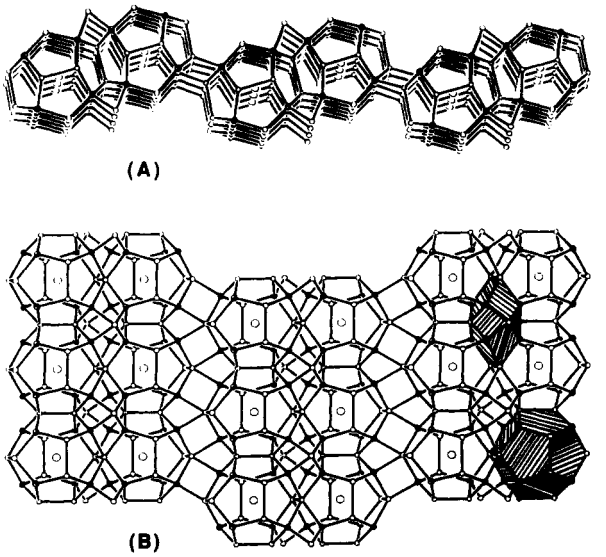

Figure 3. ORTEP representation of (A) side view of one Cu/Te layer and (B) top view of one Cu/Te layer. The $Cu_8(Te_2)_6$ and Cu_8Te_8 clusters are shaded for emphasis. Large open circles are K atoms, small open circles are Te atoms, and solid circles are Cu atoms. Selected bond distances (Å) and angles (deg) are as follows: Cu(1)–Te(2), 2.701 (2); Cu(1)–Te(4), 2.582 (1); Cu(1)–Te(5), 2.604 (2); Cu(1)–Te(8), 2.626 (2); Cu(2)–Te(2), 2.627 (1); Cu(2)–Te(6), 2.631 (2); Cu(2)–Te(6), 2.699 (1); Cu(2)–Te(7), 2.556 (1); Cu(3)–Te(1), 2.685 (2); Cu(3)–Te(3), 2.649 (2); Cu(3)–Te(4), 2.590 (1); Cu(3)–Te(9), 2.622 (1); Cu(4)–Te(1), 2.673 (2); Cu(4)–Te(3), 2.633 (2); Cu(4)–Te(7), 2.594 (1); Cu(4)–Te(9), 2.625 (1); Te(1)–Te(2), 2.812 (1); Te(3)–Te(3), 2.822 (2); Te(4)–Te(4), 2.797 (3); Te(5)–Te(6), 2.796 (1); Te(7)–Te(7), 2.797 (3); Te(8)–Te(8), 2.828 (2); Te(2)–Cu(1)–Te(4), 104.86 (4); Te(2)–Cu(1)–Te(5), 110.54 (5); Te(2)–Cu(1)–Te(8), 113.85 (6); Te(4)–Cu(1)–Te(5), 115.92 (6); Te(4)–Cu(1)–Te(8), 105.22 (5); Te(5)–Cu(1)–Te(8), 106.56 (5); Te(2)–Cu(2)–Te(6), 110.86; Te(2)–Cu(2)–Te(6), 108.76 (5); Te(2)–Cu(2)–Te(7), 110.17 (5); Te(6)–Cu(2)–Te(6), 97.52 (5); Te(6)–Cu(2)–Te(7), 117.66 (5); Te(6)–Cu(2)–Te(7), 111.02 (6); Te(1)–Cu(3)–Te(3), 103.78 (5); Te(1)–Cu(3)–Te(4), 109.09 (4); Te(1)–Cu(3)–Te(9), 116.22 (6); Te(3)–Cu(3)–Te(4), 112.47 (6); Te(3)–Cu(3)–Te(9), 109.45 (5); Te(4)–Cu(3)–Te(9), 106.00 (5); Te(1)–Cu(4)–Te(3), 105.69 (5); Te(1)–Cu(4)–Te(7), 109.28 (4); Te(1)–Cu(4)–Te(9), 117.42 (6); Te(3)–Cu(4)–Te(7), 111.82 (6); Te(3)–Cu(4)–Te(9), 109.85 (5); Te(7)–Cu(4)–Te(9), 102.91 (5).

between the layers, resulting in large channels as shown in Figure 1. The cross section of the channels is a 24-membered ring that is roughly rectangular-shaped, its short dimension at 4.581 (1) Å. The geometry around the Cu atoms is distorted tetrahedral. The average Cu–Te distance is 2.63 (4) Å, which is in the normal range of Cu–Te distances.[4-6] Short Cu–Cu contacts are also observed in this compound, ranging from 2.625 (3) Å for Cu(2)–Cu(2) to 2.810 (4) Å for Cu(1)–Cu(1). The coordination environments of Te atoms vary. The μ_4-Te(9) atoms have a square-pyramidal geometry. The tellurium atoms (Te(1), Te(2), Te(3), Te(6)) of ditellurides bond to four Cu atoms and one Te atom with a square-pyramidal geometry, whereas the tellurium atoms (Te(4), Te(5), Te(7) and Te(8)) of ditellurides bond to two Cu atoms and one Te atom with a trigonal-pyramidal geometry. Higher coordination numbers of Te atoms are also found in KCu_4TeS_2,[9] $NaCu_3Te_2$,[4] KCu_3Te_2,[5] and $TlCu_3Te_2$.[10] The average Te–Te distance of ditellurides is normal at 2.81 (1) Å.[11] There are no other short Te–Te contacts in this

(9) Park, Y.; Kanatzidis, M. G., manuscript in preparation.
(10) Klepp, K. O. *J. Less-Common Met.* **1987**, *128*, 79–89.
(11) (a) Roof, L. C.; Pennington, W. T.; Kolis, J. W. *J. Am. Chem. Soc.* **1990**, *112*, 8172–8174. (b) Adams, R. D.; Wolfe, T. A.; Eichhorn, B. W.; Haushalter, R. C. *Polyhedron* **1989**, *21*, 701–703. (c) Haushalter, R. C. *Angew. Chem., Int. Ed. Engl.* **1985**, *24*, 433–435.

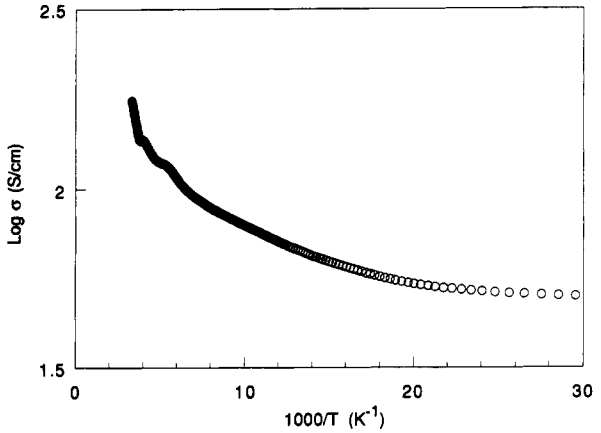

Figure 4. Four-probe electrical conductivity data as a function of temperature for a single crystal of $K_4Cu_8Te_{11}$.

compound. Selected bond distances and angles are shown in Figure 3.

There are four crystallographically distinct K atoms in this compound. The encapsulated K(1) atom is sitting slightly off-center in a rectangular plane defined by two opposite parallel ditellurides in the dodecahedral cluster. K–Te distances range from 3.676 (3) Å to 3.960 (3) Å (average of 3.75 (8) Å), and Cu–K distances range from 3.674 (3) Å to 3.724 (3) Å (average of 3.69 (7) Å). The remaining three K atoms are sitting in the tunnels with various coordination environments {8 C.N. for K(2), 10 C.N. for K(3), 6 C.N. for K(4)}. The average K–Te distances are 3.70 (16) Å for K(2), 3.66 (23) Å for K(3), and 3.71 (9) Å for K(4).

If the formal charges on the ditelluride units and monotelluride atoms are considered as −2, each Cu atoms has a formal oxidation state of +1. This suggests that $K_4Cu_8Te_{11}$ would be a semiconductor. Preliminary conductivity measurements on single crystals show a thermally activated behavior, as shown in Figure 4. However the strong deviation from linearity of the log σ vs. $1/T$ plot suggests a departure from classical semiconductor charge transport. The room-temperature conductivity is relatively high at ~160 S/cm.

The 20-vertex dodecahedral $Cu_8(Te_2)_6$ cluster and 16-vertex Cu_8Te_8 cluster are unique and, to the best of our knowledge, have no analogues in metal cluster chemistry. However, there is one 20-vertex dodecahedral cluster known, in organic chemistry, the dodecahedrane $C_{20}H_{20}$.[12] It is possible that the driving force for the stabilization of $Cu_8(Te_2)_6$ cluster is the encapsulation of the K ion. One could envision the possibility of building up novel extended structures in two or three dimensions based on this dodecahedral $Cu_8(Te_2)_6$ cluster by sharing more or all the ditelluride edges. We are expecting more of this structural motif in the Cu/Te system and further explorations with A_2Te_x/Cu suggest that this is indeed the case.[13]

Acknowledgment. Financial support from the National Science Foundation for a Presidential Young Investigator Award, CHE-8958451, is gratefully acknowledged. The X-ray instrumentation used in this work was purchased in part with funds from the National Science Foundation (CHE-8908088). We thank Don C. DeGroot for electrical conductivity measurements. This work made use of the SEM facilities of the Center for Electron Optics at Michigan State University.

(12) Ternansky, R. J.; Balogh, D. W.; Paquette, L. A. *J. Am. Chem. Soc.* **1982**, *104*, 4503-4504.
(13) Park, Y.; Kanatzidis, M. G., to be published.

Supplementary Material Available: Tables of atomic coordinates of all atoms and anisotropic and isotropic thermal parameters of all non-hydrogen atoms, bond distances and angles, and calculated and observed X-ray powder diffraction patterns (21 pages); a listing of calculated and observed ($10F_o/10F_c$) structure factors (15 pages). Ordering information is given on any current masthead page.

Dynamic Atomic-Level Observation of Staging Phenomena in Silver and Mercury Intercalates of Titanium Disulfide

M. McKelvy,*,† R. Sharma,† E. Ong,‡ G. Burr,§ and W. Glaunsinger§

Center for Solid State Science
Arizona State University, Tempe, Arizona 85287-1704
Manuel Lujan, Jr. Neutron Scattering Center
MS-H805, Los Alamos National Laboratory
Los Alamos, New Mexico 87545
Department of Chemistry, Arizona State University
Tempe, Arizona 85287-1604

Received May 7, 1991
Revised Manuscript Received July 29, 1991

Intercalation can be used to tailor the chemical and physical properties of layered compounds, resulting in a complete range of property modifications from subtle to extreme and compounds with important applications.[1-8] A general feature associated with property modifications and many applications is the effective dimensionality of the host. In this regard, staging is of fundamental significance.[6,8-10]

The phenomenon of staging is certainly one of the most extraordinary structural properties of intercalation compounds. Stage-*n* intercalates characteristically have *n* host layers between guest layers. These structures are generally found in hosts with relatively thin, flexible layers, such as the transition-metal dichalcogenides (TMDs) and graphite, which enhance both the elastic and electrostatic interlayer repulsive forces associated with staging.[8] Although staging has been the subject of numerous theoretical and experimental studies, it remains one of the most important and controversial subjects in this field.[6,8,11-14] A key question of current interest involves the roles of thermodynamics and kinetics in the staging process.

Substantial evidence indicates that observed stage

† Center for Solid State Science, Arizona State University.
‡ Los Alamos National Laboratory.
§ Department of Chemistry, Arizona State University.
* To whom correspondence should be addressed.

(1) Levy, F., Ed. *Intercalated Layered Materials*; D. Reidel: Dordrecht, Holland, 1979.
(2) Whittingham, M. S., Jacobson, A. J., Eds. *Intercalation Chemistry*; Academic Press: New York, 1982.
(3) Dresselhaus, M. S., Dresselhaus, G., Fischer, J. E., Moran, M. J., Eds. *Intercalated Graphite*; North-Holland: New York, 1983.
(4) Atwood, J. L., Davies, J. E. D., MacNicol, D. D., Eds. *Inclusion Compounds*; Academic Press: London, 1984.
(5) Dresselhaus, M. S., Ed. *Intercalation in Layered Materials*; Plenum Press: New York, 986.
(6) Ulloa, S. E.; Kirczenow, G. *Comments Cond. Mat. Phys.* **1986**, *12*, 181-197.
(7) Legrand, A. P.; Flandrois, S., Eds. *Chemical Physics of Intercalation*; Plenum Press: New York, 1987.
(8) Safran, S. A. *Solid State Phys.* **1987**, *40*, 183-246.
(9) Safran, S. A. In ref 7, pp 47-57.
(10) Fischer, J. E. In ref 7, pp 59-78.
(11) Miyazaki, H. *J. Mater. Res.* **1988**, *3*, 479-490.
(12) Suematsu, H.; Suda, K.; Metoki, N. *Synth. Met.* **1988**, *23*, 7-12.
(13) Kirczenow, G. *Synth. Met.* **1988**, *23*, 1-6.
(14) Cajipe, V.; Heiney, P. A.; Fischer, J. E. *Phys. Rev. B* **1989**, *39*, 4374-4385.

0897-4756/91/2803-0783$02.50/0